Targeting Heat Shock Proteins on Cancer Cells: Selection, Characterization, and Cell-Penetrating Properties of a Peptidic GRP78 Ligand†

Youngsoo Kim,[‡,§] Antonietta M. Lillo,[‡,§] Sebastian C. J. Steiniger,[§] Ying Liu,[§] Carlo Ballatore,[∥] Andrea Anichini,[⊥] Roberta Mortarini,[⊥] Gunnar F. Kaufmann,[§] Bin Zhou,[§] Brunhilde Felding-Habermann,[#] and Kim D. Janda*[,§,△]

The Skaggs Institute for Chemical Biology and Departments of Chemistry and Immunology, Worm Institute of Research and Medicine (WIRM), and Department of Molecular and Experimental Medicine, The Scripps Research Institute, 10550 North Torrey Pines Road, La Jolla, California 92037, Acidophil, LLC, Suite 250, 10835 Road to the Cure, San Diego, California 92121, and Department of Experimental Oncology, Istituto Nazionale per lo Studio e la Cura dei Tumori, Via Venezian 1, 20133 Milan, Italy

Received February 7, 2006; Revised Manuscript Received May 9, 2006

ABSTRACT: Peptidic ligands can be used for specific cell targeting and the delivery of payloads into the target cell. Here we describe the screening of a pool of cyclic peptide phage display libraries using whole-cell panning against human melanoma cell line Me6652/4. This strategy resulted in the selection of the cyclic 13-mer Pep42, CTVALPGGYVRVC, which showed preferential internalization into melanoma cell line Me6652/4 versus the reference cell line Me6652/56. This translocation is a receptor-mediated process that does not require electrostatic interactions nor does it involve transfer to the lysosomal compartment. The cellular receptor for Pep42 was identified as the surface membrane form of glucose-regulated protein 78 (GRP78), a member of the heat shock protein family and a marker on malignant cancer cells. The cellular uptake and intracellular trafficking of Pep42−Quantum Dot conjugates was monitored by confocal laser microscopy, and colocalization within the endoplasmic reticulum was observed. The uptake of Pep42 could be blocked by a monoclonal antibody against the identified receptor. Furthermore, Pep42 was shown to target specifically GRP78-expressing cancer cells. The in vitro cytotoxicity of a Pep42−Taxol conjugate was evaluated by flow cytometry wherein the conjugate was shown to induce apoptosis and was more effective in promoting programmed cell death in Me6652/4 cells. In summary, the data presented suggest that cyclic peptide Pep42 might be a powerful tool in the construction of drug conjugates designed to selectively kill malignant cancer cells.

Peptidic ligands with cell-penetrating properties can be used for specific cell targeting and delivery of a payload; however, the mechanistic details of cellular peptide uptake remain cryptic (*1*−*5*). Recently, peptidic ligands have gained increasing attention; it has been shown that these peptides can serve as powerful molecular tools in the treatment of cancer patients (*6*, *7*). Current chemotherapy is often limited by severe side effects induced by standard anticancer drugs, leaving patients under extreme distress. To increase the delivery efficiency and to decrease unwanted and potentially harmful and undesirable side effects, it is essential to develop methodologies that allow for the cell-specific delivery of therapeutic agents (*8*, *9*). Therefore, the discovery of peptides that specifically target cancer cells and are able to deliver a payload into these cells or a specific cellular compartment is of paramount importance (*6*). Notably, there have been several reports of peptides with such potential therapeutic properties (*10*), including cyclic peptides that display an increased biological activity over their linear analogues (*11*−*14*).

Heat shock proteins (HSP)[1] are a set of chaperone proteins involved in numerous intra- and intercellular processes, including protein synthesis and folding, vesicular trafficking, and antigen processing and presentation (*15*). Glucose-regulated protein 78 kDa [GRP78; also known as the

† This work was supported by The Skaggs Institute for Chemical Biology, the NIH (Grants AI47127, A41986, and HL63651 to K.D.J. and Grant CA112287 to B.F.H.), the California Cancer Research Program (Grant 00-00757V-20012 to K.D.J.), the California Breast Cancer Research Program (Grant 4JB-001 to K.D.J. and Grant 10YB-0202 to B.F.H.), and the Louis R. Jabinson Fellowship (Louis R. Jabinson Investigatorship Fund for Graduate Education).

* Corresponding author. E-mail: kdjanda@scripps.edu.

‡ These authors contributed equally.

§ The Skaggs Institute for Chemical Biology and Departments of Chemistry and Immunology, The Scripps Research Institute.

∥ Acidophil, LLC.

⊥ Istituto Nazionale per lo Studio e la Cura dei Tumori.

Department of Molecular and Experimental Medicine, The Scripps Research Institute.

△ Worm Institute of Research and Medicine (WIRM), The Scripps Research Institute.

[1] Abbreviations: GRP78, glucose-regulated protein 78 kDa; HSP, heat shock proteins; BiP, immunoglobulin heavy chain binding protein; FITC, fluorescein isothiocyanate; NaN_3, sodium azide; Tat, trans-acting activator of transcription; LL-37, human host defense peptide; Bpa, L-*p*-benzoylphenylalanine; QD, Quantum Dot; HDFa, human dermal fibroblast, adult; ER, endoplasmic reticulum; PBS, phosphate-buffered saline; DMEM, Dulbecco's modified Eagle's medium; FACS, fluorescent activated cell sorting; RPMI, Rosewell Park Memorial Institute; EDTA, ethylenediaminetetraacetic acid; TEA, triethylamine; HPLC, high-performance liquid chromatography; DIC, differential interference contrast; SB, super broth.

10.1021/bi060264j CCC: $33.50
Published on Web 07/01/2006

immunoglobulin heavy chain binding protein (BiP)], a member of the HSP70 family, is constitutively expressed and located in the endoplasmic reticulum (ER) of almost all cell types. However, stressful conditions lead to an increase of its expression level (*17*, *18*) and the presence of a surface membrane-bound form of GRP78. It has also been demonstrated that this overexpression of GRP78 is linked to a greater degree of malignancy in cancer cells (*19*, *20*). In addition, GRP78 induction has been correlated with the development of resistance to various cytotoxic agents (*21*, *22*). Taken together, GRP78 is an attractive target receptor of cancer cells and for utilization as a drug delivery receptor (*23*).

We have focused our attention on the discovery of peptides that specifically bind to and are internalized into cancer cells (*24*, *25*). In our current effort we prepared and utilized a set of cyclic peptide libraries expressed on the pIX coat protein of M13 filamentous phage that were screened against melanoma cells using whole-cell phage panning methodology. Two human melanoma cell lines that had been previously selected and characterized on the basis of their adhesive, invasive, and migratory abilities were panned against the highly metastatic clone Me6652/4 as a target cell line and the low metastatic clone Me6652/56 as a reference, respectively (*26*, *27*).

EXPERIMENTAL PROCEDURES

Cell Cultures. The human melanoma cells Me6652/4 and Me6652/56 (Istituto per lo Studio e la Cura dei Tumori, Milano) were cultured in subconfluent monolayers in T-75 culture flasks (Corning Inc., Corning, NY) containing RPMI 1640 medium (Gibco, Carlsbad, CA) supplemented with 10% FCS. HDFa cells were maintained in medium 106 (Cascade Biologics, Portland, OR) with 10% low serum growth supplement (Cascade Biologics). Cells were used 24 h postseeding, and the growth medium was changed 1 h before the experiment. All cells were cultured at 37 °C in a humidified atmosphere with 5% CO_2.

Whole-Cell Panning. Phage library panning was conducted as described elsewhere (*28*). In short, before each round of panning, the library was subtracted with low-metastatic Me6652/56 cells. Either a mixture of peptide phage libraries or the 13-mer peptide phage library ($\sim 5 \times 10^{12}$ cfu) was first incubated with $\sim 10^8$ cells in 10 mL of culture medium for 1 h at 4 °C. The unbound peptide phage sublibrary was added to a culture of Me6652/4. The cells were incubated for 1 h at 37 °C to allow uptake and subsequently washed five times with 10 mL of PBS, trypsinized for 7 min with 1.5 mL of trypsin−EDTA (Gibco), and resuspended in 10 mL of PBS. The cells were collected by centrifugation and washed three times for 5 min at room temperature with 5 mL of low pH buffer (200 mM glycine, 250 mM NaCl, pH 2.2) and five more times with PBS. Internalized phage was recovered by lysing the washed cells with 200 μL of 100 mM TEA followed by neutralization with 50 μL of 2 M Tris-HCl, pH 7.4. The internalized phage (TEA lysates) was incubated with 10 mL of *Escherichia coli* ER2537 (New England Biolabs, Ipswich, MA). The infected cells were collected by centrifugation (3000 rpm for 5 min), resuspended in 500 μL of medium, plated on large (150 × 15 mm; Becton Dickinson) SOBAG plates, and incubated at 37 °C overnight. On the next morning, the plates were scraped with 1 mL of SB medium supplemented with 15% glycerol, and 100 μL of the resulting suspension was used to inoculate 20 mL of SB medium supplemented with 2% glucose, 20 mM $MgCl_2$, and 100 μg/mL carbenicillin. The culture was incubated at 37 °C and the phagemid rescued by addition of 100 μL of VCSM13 helper phage ($\sim 1 \times 10^{11}$ pfu/mL; Stratagene, La Jolla, CA) followed by incubation at 37 °C for 30 min without shaking and an additional 30 min incubation at the same temperature with agitation. After this incubation step the cells were collected by centrifugation (3000 rpm for 15 min), resuspended in 100 mL of SB supplemented with 20 mM $MgCl_2$, 100 μg/mL carbenicillin, and 79 μg/mL kanamycin, and incubated at 28 °C overnight with shaking. The peptide−phage was purified by two rounds of standard PEG precipitation (*29*).

Peptide Synthesis. All of the peptides were prepared by stepwise solid-phase peptide synthesis protocols for Fmoc chemistry using DIC/HOBt as previously described (*30*). All Fmoc amino acids were obtained from Senn Chemicals (Dielsdorf, Switzerland). Boc-amino-oxyacetic acid (Aoa) was from Novabiochem (San Diego, CA). TentaGel HL NH_2 resin was from RAPP Polymere GmbH (Baden-Wuerttemberg, Germany) at a loading of 0.46 mmol of NH_2/g (100−200 mesh). Side chain protections were as follows: Arg (Pbf); Cys (Xan); Tyr (tBu); Lys (Alloc); Thr (tBu); all other amino acids were incorporated without side chain protection. Trifluoroacetic acid (Biograde) was from Halocarbon (River Edge, NJ), *N*,*N*-dimethylformamide (BioAnalyzed) was from J. T. Baker (St. Louis, MO), 6-Cl-HOBt was from Peptide International (Louisville, KY), *N*,*N*-diisopropylethylamine, *N*,*N*′-diisopropylcarbodiimide (DIC), fluorescein isothiocyanate, isomer 1, 90% (FITC), piperidine, levulinic acid, EDCI, NHS, and $Pd(PPh_3)_4$ were from Aldrich (Milwaukee, WI), and CarboxyLink coupling gel was from Pierce (Rockford, IL). All other reagents, solvents, and chemicals were of the highest purity commercially available and were used as received. RP-HPLC was performed by employing binary gradients of solvents A and B, where solvent A is 0.1% TFA in water and solvent B is 0.09% TFA in acetonitrile. Analytical RP-HPLC was performed using a Vydac 214TP5415 column at a flow rate of 1 mL/min, with detection at 214 nm during a linear gradient of 20−80% solvent B over 30 min. Preparative RP-HPLC was performed using a Vydac 214TP101522 column at a flow rate of 10 mL/min, with detection at 220 nm during a linear gradient of 20−55% solvent B over 30 min. In all cases, fractions were analyzed off-line using an ABI/Sciex 150EX single quadruple mass spectrometer and judged for purity after a consistent summing of 20 scans in multichannel analysis (MCA) mode, using the $[M + 2]^{2+}$ charged species. For preparative purification purposes, fractions that contained no single $[M + 2]^{2+}$ charged species which accounted for more than 10% of the total ion intensity were designated "pure" and pooled; the homogeneity of this pool was verified by analytical RP-HPLC and was >96%. For a more detailed description, see Supporting Information.

Confocal Laser Scanning Microscopy Analysis on Fixed and Permeabilized Cells. Me6652/4 or Me6652/56 cells were trypsinized with trypsin−EDTA (Gibco), resuspended in RPMI 1640/10% FCS, and counted. Cells (4×10^6) in 10

mL of medium were poured in 50 mL falcon tubes and left to recover for 1 h at 37 °C on an oscillatory shaker. Fluorescein-labeled Mut42 (60 μM) was then added and the incubation continued for an additional 2 h. For phage-displayed Pep42 (phage−Pep42), ~10^{11} cfu of phage−Pep42 or wild-type M13 phage (VCSM13; Stratagene) was then added and the incubation continued for an additional 2 h. The cells were collected by centrifugation (2000 rpm for 2 min), washed two times with PBS, trypsinized, washed ten times with the growth medium, washed once with PBS, resuspended in 100 μL of PBS, and cytospun onto microscope slides (Becton Dickinson, Rockville, MD) or plated on coverslips (cover glass no. 1; Corning). The adherent cells were then either fixed and permeabilized with 95% ethanol for 5 min or fixed with 4% PFA and not permeabilized, washed once with PBS, and blocked with BSA (10% in PBS, 1 h incubation). The wash-resistant phage was stained with mouse anti-M13 (Amersham Pharmacia, Piscataway, NJ; 1:100 diluted in 10% BSA, 1 h incubation, seven PBS washes) and goat anti-mouse-FITC (Pierce; 1:100 diluted in 10% BSA, 1 h incubation, seven PBS washes). The nucleus was stained by adding propidium iodide (Sigma, St. Louis, MO; diluted to 0.01 mg/mL). The cells were washed ten times with PBS and sealed with a coverslip upon addition of Antifade solution (Slow FadeAntifade; Molecular Probes, Eugene, OR). The slides were observed with a laser scanning confocal microscope (MRC1024; Bio-Rad, Hercules, CA). For quantitation of the cell-associated fluorescence, a group of at least five cells per image was selected, and the mean intracellular fluorescence intensity for each cell, with associated relative standard deviations, was determined using the Image J software package.

Confocal Laser Scanning Microscopy Analysis on Live Cells. Me6652/4 or Me6652/56 cells were detached with Trypsin-EDTA, resuspended in RPMI-1640/10% FCS and counted. Aliquots of 4×10^5 cells in 1 mL of medium were poured in a 6-well plate and allowed to recover for 1 h at 37 °C on an oscillatory shaker. Fluorescein labeled Mut42 was then added to a final concentration of 60 μM and the incubation continued for two more hrs. The cells were then transferred to Eppendorf tubes and collected by centrifugation (2000 rpm, 2 min), washed 5 times with growth medium and once with PBS, resuspended in 30 mL PBS, poured onto polylysine-coated glass bottom Petri dishes (P35 GC-0-10-C Mattek Corp.) and immediately observed by confocal laser microscopy. Quantitation of cell-associated fluorescence was determined as described above. For quantum dot uptake analysis Me6652/4 or Me6652/56 were detached with Versene (Gibco), resuspended in supplemented RPMI and counted. The required cell number was plated out on glass bottom Petri dishes. Cells were incubated with Mut42−QD and subjected to microscopy. Mut42−QD concentration was 6 μM. Due to a high-intensity signal of QD that overpowered other stains such as DAPI and PI, serial dilutions of Mut42−QD were tested and it was determined that 6 μM generated an appropriate level of fluorescence for quantitation. Dead cells were stained with PI.

Conjugation of Quantum Dots to Pep42 and Uptake Studies. Quatum Dots (Qdots 525, Quantum Dot Corp., Hayward, CA) were coupled to the peptide using a modified protocol provided by the manufacturer. EDC was purchased from Sigma. In brief, 50 μL of carboxyl Quantum Dots 525 (stock, 8 μM) was diluted to 1 μM using 10 mM borate buffer, pH 7.4. The peptide was dissolved in DMSO (stock, 10 mg/mL), and 100 μL was added to the Quantum Dots. Finally, the cross-linker EDC was dissolved in H_2O (10 mg/mL) and 57 μL of this stock solution added to the Quantum Dot peptide mixture. The mixture was stirred overnight and purified with a NAP-5 (Amersham, Piscataway, NJ) spin column. To block peptide uptake, the cells were incubated with different concentrations of anti-GRP78 mAb (BD Biosciences, San Jose, CA), namely, 0.05, 0.5, and 5 μg/mL final concentration. The cells were then washed and incubated with the Mut42−QD conjugate. The Mut42−QD concentration was 6 μM. QD was also conjugated to the scrambled sequence peptide of Mut42, CGVTPVGARYLKC (SCR42), in 6 μM.

Identification of Receptors Interacting with Pep42. To identify cell surface receptors interacting with Pep42, Me6652/4 and Me6652/56 cells (approximately 5×10^7−10^8 cells/cell line) were pretreated with 1% sodium azide (NaN_3, 99%) (Aldrich; 19,993-1) for 30 min at 37 °C. After incubation at 4 °C for 0.5−1 h, pretreated cells were interacted with 50 μM Pep42−Bpa for 1 h at 4 °C in the dark to avoid unnecessary activation. After irradiation at wavelength 320 nm with ultraviolet rays for 15 min, cells were scraped off and lysed in RIPA buffer (150 mM NaCl, 10 mM Tris-HCl, pH 7.4, 5 mM EDTA, 1% Triton X-100), supplemented with 1:100 protease inhibitor cocktail (Sigma) and 1:100 phosphatase inhibitor cocktail set II (Calbiochem; 524625). Centrifugation was performed at 10000*g* for 20 min at 4 °C, the supernatant was collected, and protein concentrations were determined using the Bradford assay (Bio-Rad, Richmond, CA). Aliquots containing 50 μg of total proteins were analyzed by 12% SDS−PAGE, followed by western blotting using streptavidin−horseradish peroxidase (HRP) (Amersham Pharmacia Biotech; RPN1231V). At the same time, biotin-labeled peptides interacting with cell surface proteins were enriched from the rest of the supernatant by avidin affinity chromatography. Avidin (100 μL, monomeric) high-capacity (HC) agarose (Sigma) equilibrated with PBS, pH 7.4, was transferred to a microcentrifuge tube. To block nonexchangeable biotin binding sites, 400 μL of a 1 mg/mL biotin solution prepared in PBS was added to the resin and incubated for 30 min at room temperature. Then, 500 μL of 0.1 M glycine, pH 2.0, was added to elute biotin from the exchangeable binding sites. The supernatant was applied to the resin and incubated for 17 h at 4 °C to facilitate optimal binding. The bound biomolecules were eluted with 2 mM biotin in PBS. The elution was analyzed by SDS−PAGE with silver stain. Two major bands were excised for further receptor identification. Gel slices were destained using washes of 50% ACN/50 mM ammonium bicarbonate until clear and dried in a centrifugal evaporator. Approximately 3 μL of sequencing grade modified trypsin (Promega) (100 ng/μL in nanopure H_2O) was added, followed by enough digestion buffer (10 mM ammonium bicarbonate/10% ACN) to cover each piece when fully rehydrated and then incubated overnight at 37 °C. Next, 8 μL of this solution was analyzed by nanoflow LC-MSMS using an Agilent 1100 nanoflow LC system coupled to an Agilent 1100 ion trap. Peptides and their collisionaly induced fragments were searched against theoretically derived protein digests and fragmentation patterns in the nonredundant protein database (NCBI)

using a licensed version of Mascot (http://www.matrixscience.com/).

Binding and Internalization Assay by FACS Analysis. Me6652/4 or Me6652/56 cells were detached for binding assays or kept adherent for internalization assays. In general, $\sim 2 \times 10^5$ cells/mL were either not pretreated or preincubated at 4 °C or at 37 °C in the presence of either 1 mM chloroquine (diphosphate salt; Sigma), 10 mM methyl-β-cyclodextrin (Fluka, Buchs SG, Switzerland), 0.1% NaN_3 (Sigma), or 50 units/mL heparin (sodium salt; Sigma). The cells were then incubated with synthetic Pep42−FITC (several concentrations of Mut42 in DMSO) at 4 °C (binding curve on untreated cells) or at 37 °C (internalization curve on untreated cells or internalization inhibition on treated cells). For the analysis of phage−Pep42 binding, the cells (2 mL) were collected by centrifugation (1000 rpm for 2 min), washed with 10 mL of ice-cold medium, resuspended in 700 μL of medium containing mouse anti-M13 antibody, and incubated on ice for 1 h. The cells were then washed as described above, resuspended in 700 μL of medium containing goat anti-mouse FITC conjugate, and incubated on ice for 1 h. Once again, the cells were washed, resuspended in medium containing propidium iodide, and immediately analyzed (FACScan; Becton Dickinson). For the synthetic Pep42−FITC binding curve, cells (10×2 mL) were collected by centrifugation (1000 rpm for 2 min), washed with 10 mL of ice-cold medium, resuspended in 700 μL of medium containing propidium iodide, and immediately analyzed. The fluorescence shifts were plotted against the corresponding concentrations of Pep42−FITC (GraFit 5; Erithacus Software Ltd., U.K.). For synthetic Pep42−FITC internalization analysis (internalization curve or effect of low temperature and chemicals) cells were placed on ice, washed five times in the wells of a six-well plate with 2 mL of ice-cold medium, and lifted. The cells were then resuspended, collected by centrifugation, washed once with medium, resuspended in 500 μL of medium containing 5 μL of trypan blue (0.4% solution; Sigma), and analyzed immediately. The fluorescence shifts were either plotted against relative concentration of synthetic peptide (Enzyme Kinetic fit in GraFit 5) or graphed in a bar graph against the pretreatment conditions (Column Chart fit in GraFit 5).

FACS Analysis of GRP78 Expression. Me6652/4 or Me6652/56 cells were detached with trypsin−versene (Cambrex Corp., East Rutherford, NJ), centrifuged, and resuspended in TBS containing 10 μg/mL mouse anti-GRP78 (Beckton Dickinson, San Jose, CA) (purified to antibody homogenicity) to a concentration of 2×10^5 cells/mL. The cells were incubated on ice for 45 min, washed once in 500 μL of TBS, resuspended in 50 μL of TBS containing 10 μg/mL goat anti-mouse-FITC (Invitrogen, Carlsbad, CA), and incubated on ice for 45 min. After one wash in 500 μL of TBS, the cells were resuspended in 500 μL of TBS containing propidium iodide and immediately analyzed (FACScan; Becton Dickinson).

Synthesis of Peptide−Taxol Conjugates. Preparative RP-HPLC purification was conducted on YMC-Pack ODS-A columns (S-5 μM, 300×20 mm i.d.) with gradient elution between 0% solvent B to 100% solvent B (solvent A = 0.05% TFA in H_2O; solvent B = 0.05% TFA in CH_3CN) with gradient times of 10 min and a flow rate of 25 mL/min with UV 220 nm detection. Analytical HPLC-MS was conducted on a YMC Combi-Screen ODS-A column (S-5 μM, 50×4.6 mm i.d.) with gradient elution of 0% solvent B to 100% solvent B (solvent A = 0.05% TFA in H_2O; solvent B = 0.05% TFA in CH_3CN) with gradient times of 10 min and a flow rate of 3.5 mL/min with UV 220 nm and Electrospray MS detection. Additional analytical HPLC was conducted on a Thomson PFP column (60A, 5 μm, 150×4.6 mm i.d.) with gradient elution of 30% solvent B to 95% solvent B (solvent A = 0.05% TFA in H_2O; solvent B = 0.05% TFA in CH_3CN) with gradient times of 10 min and a flow rate of 1.0 mL/min with UV 220 nm and UV 254 nm detection. For a detailed description, see Supporting Information.

Apoptosis Assay. Me655/2/4 and Me655/2/56 cells were seeded in medium plus 10% FCS. After 24 h, this medium was replaced with medium containing 1% FCS with or without the Mut42−Taxol conjugate (DH402 in Supporting Information), linear Lin42−Taxol (DH403 in Supporting Information), Mut42, or free Taxol, all at a concentration of 4×10^{-5} M. Apoptosis was evaluated after 72 h by flow cytometry using the Annexin V−FITC kit (BD Biosciences, PharMingen, San Diego, CA) as described (*31*). Percentages of live and apoptotic cells were determined on the basis of negative controls obtained by staining controls only with PI or only with Annexin V.

RESULTS AND DISCUSSION

Whole-Cell Panning and Selection of Pep42. A pool of phage-displayed cyclic peptide libraries was screened to select peptides that specifically target melanoma cancer cells. The basic structure of these cyclic peptide libraries was CX_nC (C = cysteine, X = any amino acid residue, $n = 3-12$). The highly metastatic melanoma clone Me6652/4 and the low metastatic clone Me6652/56 were chosen as positive and negative cell lines, respectively. A subtractive panning strategy was applied, in which the phage were first adsorbed onto reference cells before the supernatant of this reaction was transferred to the target melanoma cells, Me6652/4. The phage titer during the selection process increased 7-fold, an indication of enrichment of binding phage. After five rounds of selection, 15 clones were picked and analyzed to assess the diversity of the selected peptide sequences. DNA sequencing of the 15 clones revealed that 9 clones were identical. The corresponding predominant peptide sequence was the cyclic 13-mer CTVALPGGYVRVC, denoted Pep42. A database search using the amino acid sequence (BLASTP, search of short, nearly exact matches) revealed no significant matches or any specific motifs. However, it is still possible that the identified peptide shares a motif with a yet unidentified protein.

Cellular Uptake of Pep42 by Melanoma Cells. To study the uptake and intracellular localization of Pep42, we synthesized the peptide by replacing the valine at position 12 with a lysine residue in order to conjugate a fluorescein isothiocyanate (FITC) moiety. This derivative was named Mut42 and had the following sequence: CTVALPGGYVRKC (Figure 1A). Incubation of melanoma cells with the Mut42−fluorescein conjugate confirmed that the internalization was more efficient in the Me6652/4 cells compared to the control Me6652/56 cells (Figure 1B). To exclude fixation artifacts as a reason for the observed peptide uptake,

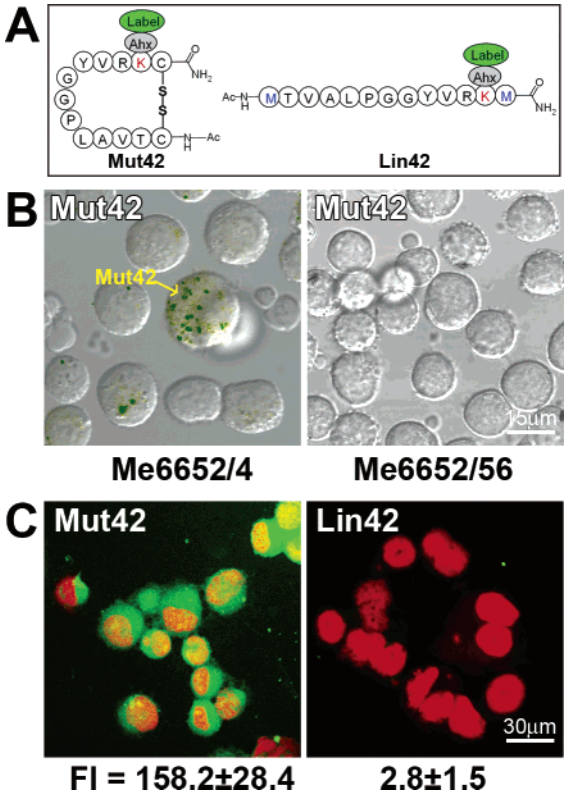

FIGURE 1: Variants of Pep42 and internalization of Pep42 variants in melanoma Me6652/4 or Me6652/56 cells as viewed by confocal laser scanning microscopy. Label = fluorescein isothiocyanate, Quantum Dots, or Taxol; Ahx = aminohexanoic acid; Ac = acetyl group. (A) Synthetic variants of Pep42. (B) The cells were incubated with fluorescein-labeled Mut42 (green). The cells were neither fixed nor permeabilized and viewed by differential interference contrast (DIC) with merging images from the green fluorescent channel. (C) Me6652/4 cells were incubated with fluorescein-labeled Mut42 or Lin42 (green), fixed, permeabilized, and stained with propidium iodide (PI) (nuclear and partial cytoplasm stain, red).

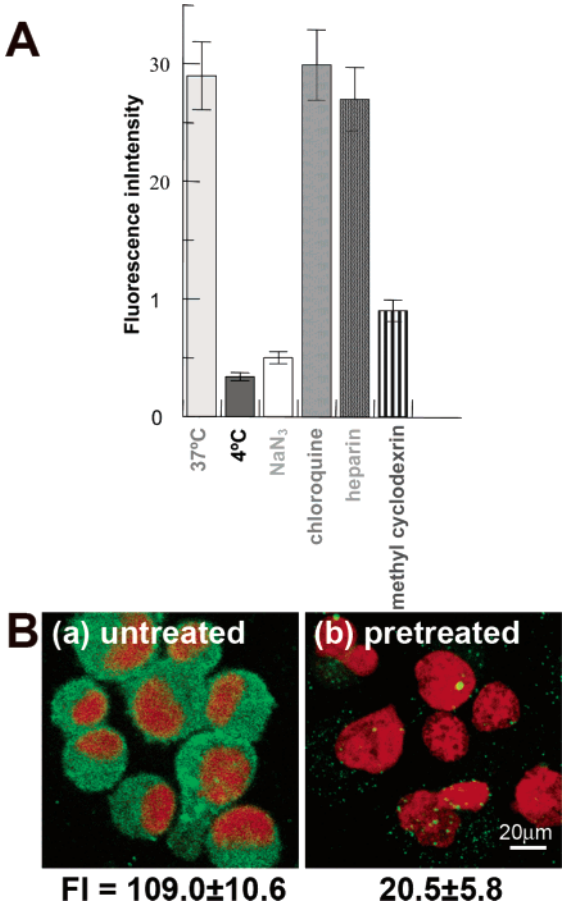

FIGURE 2: Quantitative flow cytometry analysis of Mut42 internalization. (A) Me6652/4 cells were either untreated (control) or pretreated by prolonged exposure at 4 °C or by incubation with either 1% NaN_3, 1 mM chloroquine, 50 units/mL heparin, or 10 mM methyl-β-cyclodextrin and then incubated in the presence of 100 μM fluorescein-labeled Mut42 for 1 h at 37 °C. External binding was removed by trypsinization, and the cells were analyzed immediately after addition of PI. (B) Me6652/4 and Me6652/56 cells were either (a) untreated or (b) pretreated with methyl-β-cyclodextrin and then incubated with fluorescein-labeled Mut42 and stained as described above. FI = fluorescence intensity (FITC, green).

a set of experiments was designed in which live cells were used. Importantly, peptide uptake was still observed by the increase in the internal fluorescence signal. This provides strong evidence that the internalization of Pep42 into fixed cells was indeed not an experimental artifact. The cellular uptake of Mut42 indicates that N-terminal capping and the mutation V12K, required for the coupling of FITC and potentially other payloads, do not negatively affect the internalizing capability of Pep42. Notably, no internalization was observed when the cells were treated with the linear derivative Lin42 peptide (Figure 1C), demonstrating that the cyclic constraint, which is likely to provide additional structural elements to Pep42, is absolutely required for internalization. To exclude peptide uptake property alternation due to fluorescein conjugation, an additional set of experiments was designed in which phage-displayed Pep42 (phage−Pep42) were used, followed by antibody staining (see Supporting Information, S1).

Uptake and Internalization Inhibition Study by FACS. To confirm the specificity of Mut42 internalization seen in the microscopy experiments and to quantify cellular uptake, fluorescein-conjugated Mut42 was analyzed by flow cytometry under conditions that either permit internalization or prevent active uptake by live cells. In analogy to previously described binding analyses, plotting of fluorescence shifts against the corresponding peptide concentrations yielded saturation curves with maxima greater for the Me6652/4 than for the Me6652/56 melanoma cells (see Supporting Information, S2). Overall, fluorescent shifts observed in the internalization studies were smaller than those seen in the binding analyses (see Supporting Information, S3). This effect could be attributed to fluorescence quenching inside the cell (*32*−*34*). To address the mechanism of Mut42 internalization, the cells were exposed to various conditions known to inhibit endocytosis (*35*). Cellular peptide uptake was greatly reduced when incubation was performed at 4 °C (Figure 2A). Here, inhibition of endocytosis can be attributed not only to a blockade of active processes but also to the rigidification of the lipid membrane at this temperature (*36*). Therefore, peptide internalization was examined at 37 °C with or without preincubation with cytochrome oxidase inhibitor sodium azide (NaN_3), which impairs energy-dependent translocation of molecules into cells by depleting the intracellular ATP pool. Sodium azide treatment reduced the level of internalization at 37 °C to that observed at 4 °C, again indicating active

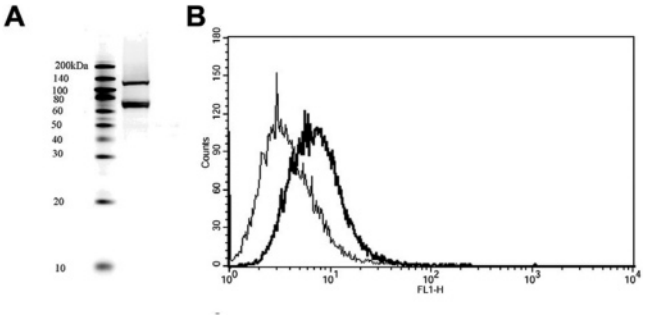

FIGURE 3: (A) Western blot of Mut42−Bpa with its interacting proteins. The Mut42-bonded proteins on the cell surface were purified by avidin−agarose affinity chromatography, separated by SDS−PAGE, and transferred onto a nitrocellulose membrane. Upon incubation with streptavidin−HRP the membrane was developed with luminol and analyzed by chemoluminescence. (B) FACS analysis of GRP78 expression. Flow cytometry of anti-GRP78 binding to either melanoma cell, Me6652/4 (bold line) or Me6652/56 (thin line). Upon treatment with the primary antibody, cells were incubated with FITC-conjugated secondary antibody and PI.

internalization as the underlying translocation mechanism (Figure 2A).

For many cationic cell-penetrating peptides, cell internalization involves electrostatic interaction with the negatively charged sulfated proteoglycans of the plasma membrane (*37*−*40*). To investigate this possibility with fluorescein−Mut42, cells were preincubated in the presence of heparin; the lack of any measurable effect provides evidence that interaction with sulfated proteoglycans is not a prerequisite for Mut42 internalization. Furthermore, pretreatment with the chloroquine, an inhibitor of lysosomal function, also failed to affect the uptake. This finding suggests that the peptide is not compartmentalized into lysosomes upon internalization. Finally, pretreatment of the cells with methyl-β-cyclodextrin strongly reduced Pep42 internalization as measured by flow cytometry (see Supporting Information, S3) and confirmed by confocal microscopy (Figure 2B). Since methyl-β-cyclodextrin is known to extract cholesterol from cell membranes (*41*), this result provides strong evidence for a potential involvement of lipid rafts (*42*−*44*). The mechanism of Pep42 uptake parallels to some extent that reported for cell-penetrating peptides like Tat (*45*) and LL-37 (*46*); however, receptor-mediated translocation is involved in Pep42 internalization.

Photoaffinity Labeling of Pep42 Detects GRP78. Since a more complex structure might facilitate specific interaction with a receptor, this finding led us to the hypothesis that Pep42 internalization is receptor-mediated. To identify cell surface receptors that interact with Pep42, a photoaffinity cross-linker, L-*p*-benzoylphenylalanine (Bpa), was used. This photoreactive amino acid has been utilized in identifying sites of interaction between a photolabile peptide ligand and its receptor by photoinsertion into C−H bonds of any adjacent amino acid (*47*). Mut42 was coupled to Bpa and biotinylated at the K-12 position (Mut42−Bpa−biotin) for detection and subsequent isolation of the covalent peptide−receptor complex. Me6652/4 cells were incubated with a Mut42−Bpa−biotin at 4 °C for 1 h, and the Bpa moiety was activated by long near-UV wavelengths (320 nm). The cell lysates were purified by avidin−agarose beads and analyzed by SDS−PAGE followed by western blot analysis. Two bands were observed, corresponding to proteins with apparent molecular masses of 80 and 130 kDa, respectively (Figure 3A). Mass spectrometry analysis identified the band at 80 kDa as GRP78, whereas no protein was identified with a significant

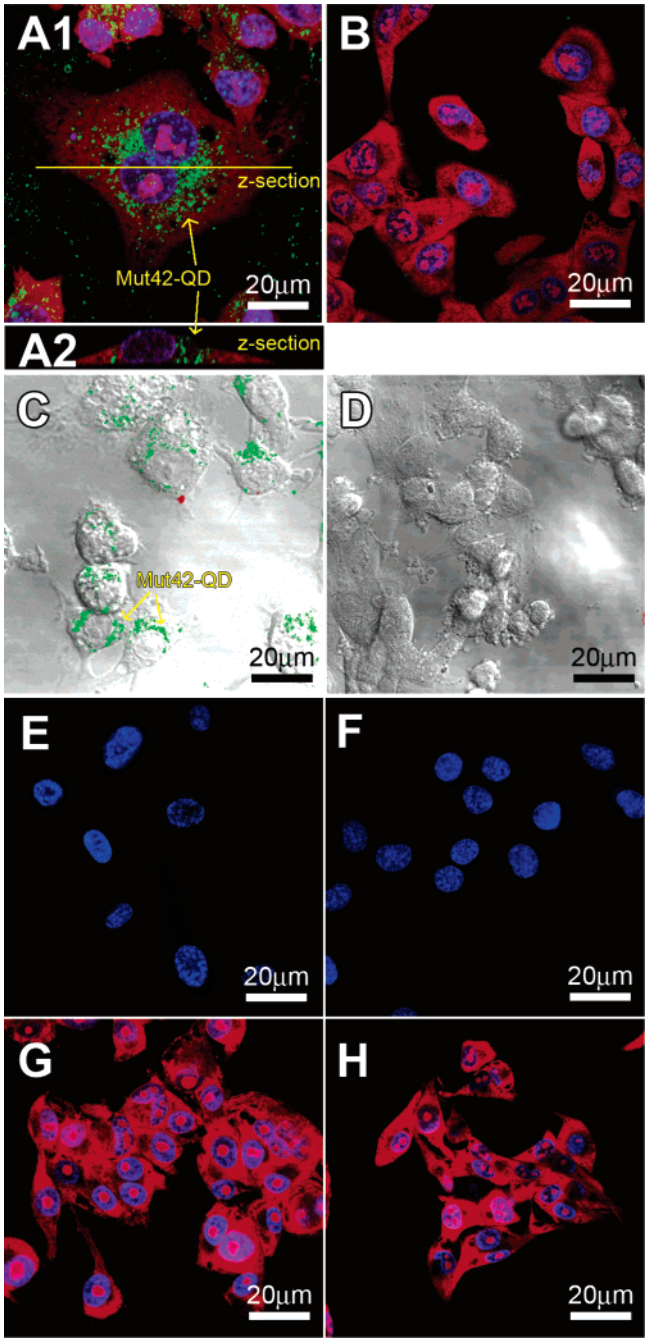

FIGURE 4: Internalization of Mut42−QD and SCR42−QD in melanoma Me6652/4 or Me6652/56 cells as viewed by confocal laser scanning microscopy. (A1) Me6652/4 cells and (B) Me6652/56 cells were incubated with Mut42−QD (green), fixed, and stained with PI (red) and DAPI (blue). (A2) *Z* cross section of sample A1 to show the localizing region of Mut42−QD. Panels A1 and A2 demonstrate that Mut42−QD is localized in the cytoplasm and does not enter the nucleus. (C) Me6652/4 and (D) Me6652/56: the cells were incubated with Mut42−QD, but neither fixed nor permeabilized, and viewed by DIC and merged with images from the green (Mut42−QD) and red (PI) fluorescent channel. (E) HDFa human fibroblast cells were incubated with Mut42−QD (green), and (F) Me6652/4 cells were incubated only with QDs, and then they were fixed and stained with DAPI (blue). (G) Me6652/4 cells and (H) Me6652/56 cells were incubated with a scrambled sequence peptide of Mut42−QD (SCR42-QD) (green), fixed, and stained with PI and DAPI. No green signal was observed in panels E−H.

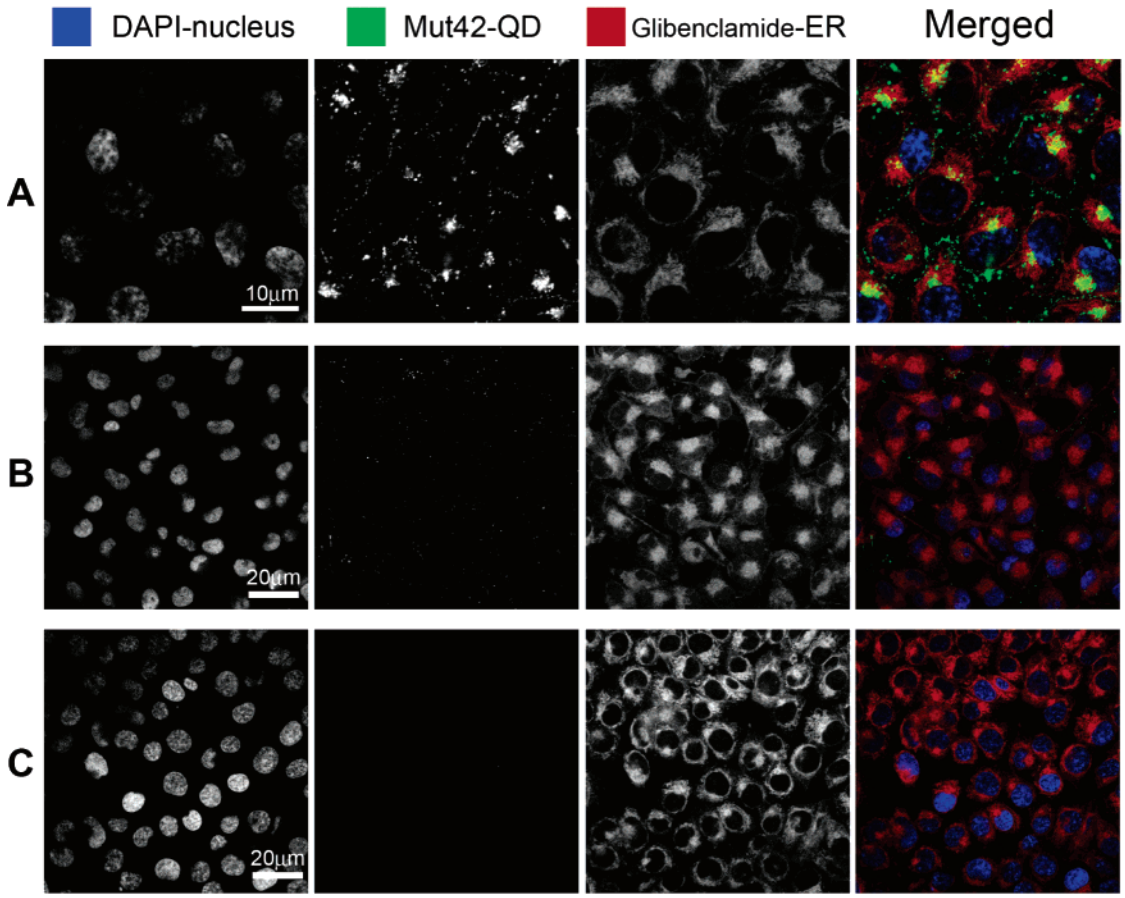

FIGURE 5: Colocalization of Mut42−QD in melanoma Me6652/4 or Me6652/56 cells as viewed by confocal laser scanning microscopy. (A) Me6652/4 cells and (B) Me6652/56 cells were incubated with Mut42−QD (green), fixed, and stained with Glibenclamide (ER and partial cytoplasm stain, red) and DAPI (blue). (C) Me6652/4 cells were incubated with only the QDs (green), fixed, and stained in the same manner above as a negative control. Mut42 is localized in the ER region.

ion score for the 130 kDa band. To serve as a receptor for Pep42, GRP78 would have to be present at the cell surface. FACS analysis of Me6652/4 and Me6652/56 cells treated with anti-GRP78 antibody confirmed that these cells indeed expressed GRP78 on their surface, resulting in a shift of the fluorescence peak relative to control IgG. As expected, the observed expression level of GRP78 was higher on the surface of Me6652/4 cells than on control Me6652/56 cells (Figure 3B). These results support the previously proposed role for GRP78 as a functional receptor for peptide ligands in vivo and a relevant molecular target expressed in metastatic tumors (*48*). We note that peptidic ligands have been identified which bind to immobilized GRP78; however, these were linear peptides and do not share any sequence similarities with Pep42 (*48*, *49*), and furthermore, the intracellular fate of these ligands has not been determined. Receptor identification by affinity chromatography was performed prior to this experiment as a pilot assay using both Me6652/56 and Me6652/4, and GRP78 was also identified as a receptor on Me6652/4 while no receptor could be found on Me6652/56 (see Supporting Information, S4).

Quantum Dot (QD) Labeled Mut42 Localizes in Perinuclear Region. The use of organic fluorophores such as fluorescein for certain applications is limited because of their inherent tendency to undergo photobleaching. In contrast, nanocrystals, like semiconductor QD, are used as stable and bright fluorophores with high quantum yields, a high absorbency, and resistance to photobleaching. To assess the intracellular distribution of Pep42 after internalization, QDs were conjugated to Mut42 (Mut42−QD). These conjugates were added to fixed and live Me6652/4 and Me6652/56 cells, and upon optical excitation, accumulation of Pep42−QD was observed in the perinuclear region of these cells (Figure 4A1,A2). The internalization of Mut42−QD and the routing to the perinuclear region were observed within 30 min (see Supporting Information, S5). Comparing the uptake of Mut42−QD into the two cell lines, a stronger signal was detected in the Me6652/4 cells (Figure 4A1,A2,C), while a weak signal was observed in the Me6652/56 cells (Figure 4B,D), and no uptake was seen in the human dermal fibroblast cell line (HDFa), which served as an additional control (Figure 4E,F). QDs were conjugated to a scrambled sequence peptide (SCR42−QD). The control peptide conjugate was added to fixed and live Me6652/4 and Me6652/56 cells, and as expected, no uptake was seen in these cell lines (Figure 4G,H). The co-incubation of cells with Mut42−QD and Glibenclamide, a biochemical marker that stains the ER, revealed that Mut42−QD colocalized with the ER (Figure 5A), which is consistent with the above observed perinuclear enrichment of Pep42−QD. No uptake and no colocalization of Pep42−QD were observed in the control cells (Figure 5B), and QD without peptide attached also did not enter the cell (Figure 5C). To exclude QD conjugation artifacts as a reason for the observed peptide uptake, a set of experiments was designed in which unconjugated Quantum Dots were used (see Supporting Information, S6). These

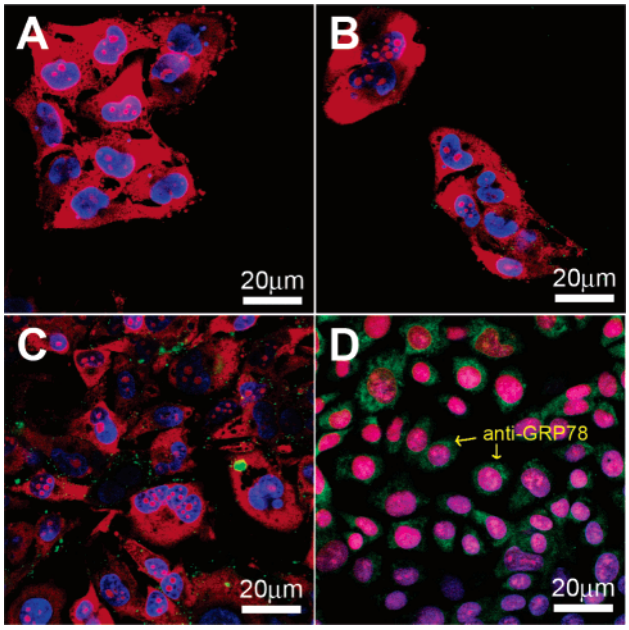

FIGURE 6: Receptor detection and internalization inhibition by anti-GRP78 antibody. GRP78 receptors on Me6652/4 were blocked by anti-GRP78 antibody in concentrations of (A) 5 μg/mL, (B) 0.5 μg/mL, and (C) 0.05 μg/mL, and cells were incubated with Mut42−QD (green), fixed, and stained with PI (red) and DAPI (blue). (D) Me6652/4 cells were incubated with anti-GRP78 antibody, fixed, and stained with a secondary FITC-conjugated antibody (green), PI (red), and DAPI (blue).

results show that Pep42 has the remarkable property to internalize selectively into Me6652/4 cells while carrying a cargo, in this case QD. The fact that HSPs are ER-resident chaperones might explain that, after binding to GRP78, the resulting complex of the peptide−conjugate and GRP78 protein colocalized with the ER. Notably, so far no cell-type specificity has been reported to date for any cell-penetrating peptide (*50*). This specificity, however, is absolutely essential to drug targeting in vivo. Furthermore, our data show that the uptake of Pep42 is specific for cells overexpressing GRP78.

Anti-GRP78 Antibody Inhibits Internalization of Pep42−QD by Cells. Several reports have shown that GRP78 is localized on the surface of cells under stressful conditions (*48*). Therefore, to study whether GRP78 is required for the internalization of Pep42, we used an anti-GRP78 monoclonal antibody to block GRP78 and, thus, to inhibit the binding and subsequent internalization of Mut42−QD. The uptake studies were carried out after preincubation of Me6652/4 cells with the monoclonal anti-GRP78 antibody. Preincubation with different concentrations of mAb prevented the cellular uptake of Mut42−QD in a concentration-dependent manner (Figure 6A−C). These results indicate that the internalization of Pep42 is mediated by GRP78 and also provides additional evidence for the specificity of the Pep42−GRP78 interaction and the presence of GRP78 on Me6652/4 cells (Figure 6D).

Induction of GRP78 Expression Leads to Increased Accumulation of Mut42−QD. It has been reported that glucose starvation of cells induces the overexpression of GRP78 (*48*). To achieve this, Me6652/56 cells were starved in glucose-free medium, and after 24 h, medium containing deoxyglucose was added to the cells, resulting in GRP78 overexpression within 2−4 h compared to noninduced control cells, as demonstrated by immuncytochemical staining (Figure 7A). The cells were then incubated with Mut42−QD, and an increased intracellular fluorescence signal was observed (Figure 7B,C). The starvation led to an overexpression of GRP78 on the cell surface which made the cells more susceptible for Mut42−QD uptake. These results provide additional evidence that the uptake of peptide is indeed receptor-mediated and GRP78 is involved in the internalization and intracellular transport of Pep42.

Mut42−Taxol Induces Apoptosis in Cells in Vitro. To evaluate the potential of Pep42 as a delivery agent of cytotoxic drugs, melanoma cells Me6652/4 and Me6652/56 were cultured for 72 h in the presence of 4×10^{-5} M Mut42−Taxol DH402 (see Supporting Information, S7), using the unconjugated Mut42 and the free Taxol (DH393; see Supporting Information, S7) as controls. Mut42−Taxol was effective in promoting apoptosis of Me6652/4 cells (92.1% of the cells in late stages of apoptosis, Figure 8), which is consistent with peptide binding and internalization, results in agreement with flow cytometry and confocal microscopy (vide supra). Furthermore, the apoptotic response of Me6652/56 cells was reduced compared to Me66652/4 cells. Importantly, a lower overall apoptotic response was observed when both cell lines were cultured in the presence of Lin42−Taxol (DH403; see Supporting Information, S7). Comparable cytotoxic effects of Lin42−Taxol and free Taxol were observed with both cell lines by flow cytometry; this suggests that Lin42−Taxol was taken up via unspecific pinocytosis. Finally, incubation of both cell lines in the presence of unconjugated Mut42 resulted in apoptosis, which paralleled the minimal extent of cell death seen in the

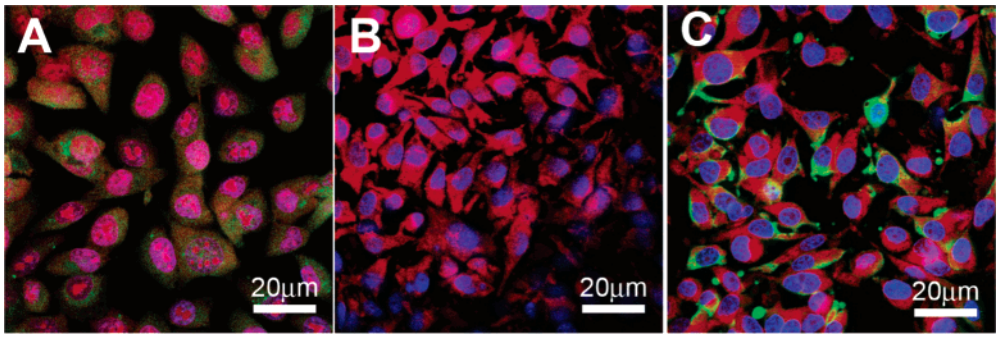

FIGURE 7: GRP78 overexpressing Me6652/56 cells as viewed by confocal laser scanning microscopy. (A) GRP78 overexpressing Me6652/56 cells were incubated with anti-GRP78 antibody and a secondary FITC-conjugated antibody (green), and (B) untreated Me6652/56 and (C) GRP78 overexpressing Me6652/56 cells were incubated with Mut42−QD (green). Cells were fixed and stained with PI (red) and DAPI (blue).

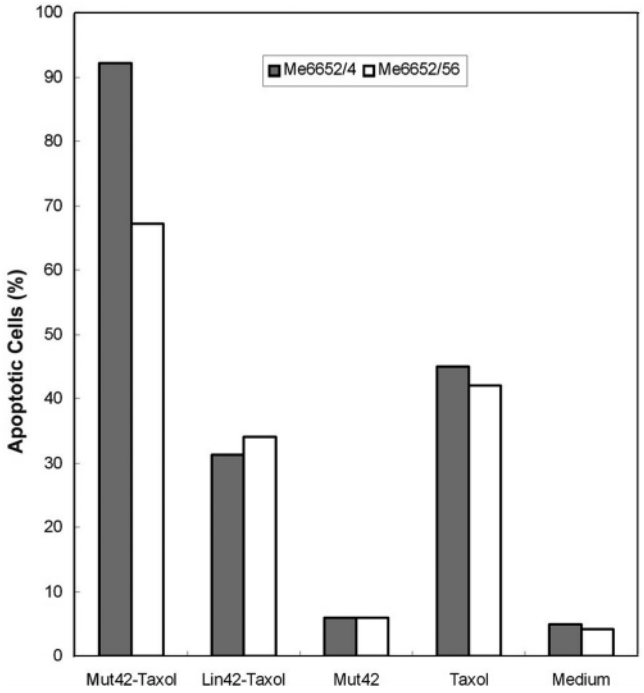

FIGURE 8: Promotion of apoptosis in melanoma clones by peptide−Taxol conjugates. Extent of late apoptosis induced by peptide−Taxol conjugates or free Taxol, all at a concentration of 4×10^{-5} M, in two melanoma clones, Me6652/4 and Me6652/56. Numbers within the *Y*-axis indicate the percentage of cells in each apoptosis experiment. Late stage apoptosis was determined by Annexin V and PI assays, and the numbers were obtained by FACS. Data shown above are from one representative apoptosis experiment out of three performed. The selection and identification of Pep42, a cyclic peptide ligand of GPR78, which internalizes selectively into highly metastatic human melanoma cells through a receptor-mediated process are reported: DAPI (blue), fluorescent peptide (green), and PI (red).

presence of growth medium. It is important to note that the cyclic Mut42−Taxol induces apoptosis more efficiently than free Taxol. In total, our data demonstrate that the melanoma cells are more sensitive to the peptide−Taxol conjugate than to free Taxol, due to the specific binding of Pep42 to the tumor cells, which facilitates drug delivery and internalization.

CONCLUSION

The binding of Pep42 to GRP78 and the subsequent internalization might be a reflection of the pathophysiological role of cell surface GRP78. Recent studies suggest that binding of ligands to GRP78 on prostate cancer cells induces mitogenic signaling and cellular proliferation and, in addition, enhances the metastatic potential of these cells (*51*, *52*). Data suggest that sera of prostate cancer patients contain autoantibodies against GRP78, and the presence of these antibodies is highly correlated with increased metastatic potential (*53*). There is also evidence that GRP78 can be targeted with peptidic ligands in vivo (*48*). The putative mechanism of the transport of the Pep42−receptor complex into the ER seems to involve the regular membrane recycling, which would then be responsible for the internalization and, thus, subsequent perinuclear localization of the peptide. Recent studies have identified the ER as an organelle that plays a major role in cellular response to stress and cellular activation of apoptosis (*54*). Therefore, Pep42 represents a promising carrier to target the ER and deliver therapeutic agents organelle specific into cancer cells.

In summary, we report the selection and identification of Pep42, a cyclic peptide ligand of GPR78, which internalizes selectively into highly metastatic human melanoma cells through a receptor-mediated process. Photoaffinity chromatography and antibody uptake inhibition studies were utilized in the identification of the Pep42 target receptor GRP78, which is a recently identified cancer cell surface antigen, thus providing cancer cell specific targeting of Pep42. The Taxol-conjugated cyclic peptide exhibited selective cytotoxicity against highly metastatic melanoma cells, as the nonspecific toxicity of anticancer drugs toward normal tissues can result in serious side effects, thereby limiting their clinical application. Taken together, our results establish the potential of Pep42 as a tool for the construction of drug conjugates designed to selectively kill malignant cancer cells while reducing side effects caused by drug interactions with normal cells.

ACKNOWLEDGMENT

The authors gratefully acknowledge David Kujawa for preparing the cell cultures and Jane Forsyth for performing the FACS analysis.

SUPPORTING INFORMATION AVAILABLE

Flow cytometry analysis of Pep42 binding and internalization, confocal microscopy of Pep42 internalization in different time frames, synthesis of Pep42 variants, synthesis of Pep42−Taxol, and receptor identification by affinity chromatography. This material is available free of charge via the Internet at http://pubs.acs.org.

NOTE ADDED AFTER ASAP PUBLICATION

This paper was published ASAP on 07/01/06. Figure 1 has been revised, and the correct version was published on 07/11/06.

REFERENCES

1. Foerg, C., Ziegler, U., Fernandez-Carneado, J., Giralt, E., Rennert, R., Beck-Sickinger, A. G., and Merkle, H. P. (2005) Decoding the entry of two novel cell-penetrating peptides in HeLa cells: lipid raft-mediated endocytosis and endosomal escape, *Biochemistry 44*, 72−81.
2. Ziegler, A., Nervi, P., Durrenberger, M., and Seelig, J. (2005) The cationic cell-penetrating peptide CPP(TAT) derived from the HIV-1 protein TAT is rapidly transported into living fibroblasts: optical, biophysical, and metabolic evidence, *Biochemistry 44*, 138−148.
3. Richard, J. P., Melikov, K., Vives, E., Ramos, C., Verbeure, B., Gait, M. J., Chernomordik, L. V., and Lebleu, B. (2003) Cell-penetrating peptides. A reevaluation of the mechanism of cellular uptake, *J. Biol. Chem. 278*, 585−590.
4. Ruoslahti, E., Duza, T., and Zhang, L. (2005) Vascular homing peptides with cell-penetrating properties, *Curr. Pharm. Des. 11*, 3655−3660.
5. Barry, M. A., Dower, W. J., and Johnston, S. A. (1996) Toward cell-targeting gene therapy vectors: selection of cell-binding peptides from random peptide-presenting phage libraries, *Nat. Med. 2*, 299−305.
6. Landon, L. A., and Deutscher, S. L. (2003) Combinatorial discovery of tumor targeting peptides using phage display, *J. Cell. Biochem. 90*, 509−517.
7. Joliot, A., and Prochiantz, A. (2004) Transduction peptides: from technology to physiology, *Nat. Cell Biol. 6*, 189−196.

8. Fennelly, D., and Schneider, J. (1995) Role of chemotherapy dose intensification in the treatment of advanced ovarian cancer, *Oncology (Williston Park) 9*, 911−921; discussion 922, 924, 926.
9. Alexandrescu, D. T., Dutcher, J. P., and Wiernik, P. H. (2005) Metastatic melanoma: is biochemotherapy the future?, *Med. Oncol. 22*, 101−111.
10. Tsuchiya, Y., Sawada, S., Tsukada, K., and Saiki, I. (2002) A new pseudo-peptide of Arg-Gly-Asp (RGD) inhibits intrahepatic metastasis of orthotopically implanted murine hepatocellular carcinoma, *Int. J. Oncol. 20*, 319−324.
11. Kato, M., and Mrksich, M. (2004) Using model substrates to study the dependence of focal adhesion formation on the affinity of integrin-ligand complexes, *Biochemistry 43*, 2699−2707.
12. Aumailley, M., Gurrath, M., Muller, G., Calvete, J., Timpl, R., and Kessler, H. (1991) Arg-Gly-Asp constrained within cyclic pentapeptides. Strong and selective inhibitors of cell adhesion to vitronectin and laminin fragment P1, *FEBS Lett. 291*, 50−54.
13. Suzuki, N., Nakatsuka, H., Mochizuki, M., Nishi, N., Kadoya, Y., Utani, A., Oishi, S., Fujii, N., Kleinman, H. K., and Nomizu, M. (2003) Biological activities of homologous loop regions in the laminin alpha chain G domains, *J. Biol. Chem. 278*, 45697−45705.
14. Gurrath, M., Muller, G., Kessler, H., Aumailley, M., and Timpl, R. (1992) Conformation/activity studies of rationally designed potent anti-adhesive RGD peptides, *Eur. J. Biochem. 210*, 911−921.
15. Macario, A. J., and Conway de Macario, E. (2005) Sick chaperones, cellular stress, and disease, *N. Engl. J. Med. 353*, 1489−1501.
16. Delpino, A., Piselli, P., Vismara, D., Vendetti, S., and Colizzi, V. (1998) Cell surface localization of the 78 kD glucose regulated protein (GRP 78) induced by thapsigargin, *Mol. Membr. Biol. 15*, 21−26.
17. Li, W. W., Alexandre, S., Cao, X., and Lee, A. S. (1993) Transactivation of the grp78 promoter by Ca^{2+} depletion. A comparative analysis with A23187 and the endoplasmic reticulum Ca(2+)-ATPase inhibitor thapsigargin, *J. Biol. Chem. 268*, 12003−12009.
18. Lee, A. S. (1992) Mammalian stress response: induction of the glucose-regulated protein family, *Curr. Opin. Cell Biol. 4*, 267−273.
19. Fernandez, P. M., Tabbara, S. O., Jacobs, L. K., Manning, F. C., Tsangaris, T. N., Schwartz, A. M., Kennedy, K. A., and Patierno, S. R. (2000) Overexpression of the glucose-regulated stress gene GRP78 in malignant but not benign human breast lesions, *Breast Cancer Res. Treat. 59*, 15−26.
20. Song, M. S., Park, Y. K., Lee, J. H., and Park, K. (2001) Induction of glucose-regulated protein 78 by chronic hypoxia in human gastric tumor cells through a protein kinase C-epsilon/ERK/AP-1 signaling cascade, *Cancer Res. 61*, 8322−8330.
21. Reddy, R. K., Mao, C., Baumeister, P., Austin, R. C., Kaufman, R. J., and Lee, A. S. (2003) Endoplasmic reticulum chaperone protein GRP78 protects cells from apoptosis induced by topoisomerase inhibitors: role of ATP binding site in suppression of caspase-7 activation, *J. Biol. Chem. 278*, 20915−20924.
22. Chatterjee, S., Cheng, M. F., Berger, R. B., Berger, S. J., and Berger, N. A. (1995) Effect of inhibitors of poly(ADP-ribose) polymerase on the induction of GRP78 and subsequent development of resistance to etoposide, *Cancer Res. 55*, 868−873.
23. Fujihara, S. M., and Nadler, S. G. (1999) Intranuclear targeted delivery of functional NF-kappaB by 70 kDa heat shock protein, *EMBO J. 18*, 411−419.
24. Kim, Y., Lillo, A., Moss, J. A., and Janda, K. D. (2005) A contiguous stretch of methionine residues mediates the energy-dependent internalization mechanism of a cell-penetrating peptide, *Mol. Pharm. 2*, 528−535.
25. Moss, J. A., Lillo, A., Kim, Y. S., Gao, C., Ditzel, H., and Janda, K. D. (2005) A dimerization "switch" in the internalization mechanism of a cell-penetrating peptide, *J. Am. Chem. Soc. 127*, 538−539.
26. Anichini, A., Mortarini, R., Fossati, G., and Parmiani, G. (1986) Phenotypic profile of clones from early cultures of human metastatic melanomas and its modulation by recombinant interferon gamma, *Int. J. Cancer 38*, 505−511.
27. Anichini, A., Mortarini, R., Supino, R., and Parmiani, G. (1990) Human melanoma cells with high susceptibility to cell-mediated lysis can be identified on the basis of ICAM-1 phenotype, VLA profile and invasive ability, *Int. J. Cancer 46*, 508−515.
28. Gao, C., Mao, S., Ditzel, H. J., Farnaes, L., Wirsching, P., Lerner, R. A., and Janda, K. D. (2002) A cell-penetrating peptide from a novel pVII-pIX phage-displayed random peptide library, *Bioorg. Med. Chem. 10*, 4057−4065.
29. Gao, C., Brummer, O., Mao, S., and Janda, K. D. (1999) Selection of human metalloantibodies from a combinatorial phage single-chain antibody library, *J. Am. Chem. Soc. 121*, 6517−6518.
30. Chan, W. C., and White, P. D. (2000) *Fmoc Solid-Phase Peptide Synthesis*, Oxford University Press, Oxford.
31. Zanon, M., Piris, A., Bersani, I., Vegetti, C., Molla, A., Scarito, A., and Anichini, A. (2004) Apoptosis protease activator protein-1 expression is dispensable for response of human melanoma cells to distinct proapoptotic agents, *Cancer Res. 64*, 7386−7394.
32. Finney, D. A., and Sklar, L. A. (1983) Ligand/receptor internalization: a kinetic, flow cytometric analysis of the internalization of *N*-formyl peptides by human neutrophils, *Cytometry 4*, 54−60.
33. Sklar, L. A. (1987) Real-time spectroscopic analysis of ligand−receptor dynamics, *Annu. Rev. Biophys. Biophys. Chem. 16*, 479−506.
34. Kwon, S., and Carson, J. H. (1998) Fluorescence quenching and dequenching analysis of RNA interactions in vitro and in vivo, *Anal. Biochem. 264*, 133−140.
35. Fotin-Mleczek, M., Fischer, R., and Brock, R. (2005) Endocytosis and cationic cell-penetrating peptides—a merger of concepts and methods, *Curr. Pharm. Des. 11*, 3613−3628.
36. Letoha, T., Gaal, S., Somlai, C., Czajlik, A., Perczel, A., and Penke, B. (2003) Membrane translocation of penetratin and its derivatives in different cell lines, *J. Mol. Recognit. 16*, 272−279.
37. Tyagi, M., Rusnati, M., Presta, M., and Giacca, M. (2001) Internalization of HIV-1 tat requires cell surface heparan sulfate proteoglycans, *J. Biol. Chem. 276*, 3254−3261.
38. Goncalves, E., Kitas, E., and Seelig, J. (2005) Binding of oligoarginine to membrane lipids and heparan sulfate: structural and thermodynamic characterization of a cell-penetrating peptide, *Biochemistry 44*, 2692−2702.
39. Lensink, M. F., Christiaens, B., Vandekerckhove, J., Prochiantz, A., and Rosseneu, M. (2005) Penetratin-membrane association: W48/R52/W56 shield the peptide from the aqueous phase, *Biophys. J. 88*, 939−952.
40. Ziegler, A., Blatter, X. L., Seelig, A., and Seelig, J. (2003) Protein transduction domains of HIV-1 and SIV TAT interact with charged lipid vesicles. Binding mechanism and thermodynamic analysis, *Biochemistry 42*, 9185−9194.
41. Ohvo, H., and Slotte, J. P. (1996) Cyclodextrin-mediated removal of sterols from monolayers: effects of sterol structure and phospholipids on desorption rate, *Biochemistry 35*, 8018−8024.
42. Simons, K., and Ikonen, E. (1997) Functional rafts in cell membranes, *Nature 387*, 569−572.
43. Brown, D. A., and London, E. (1998) Functions of lipid rafts in biological membranes, *Annu. Rev. Cell Dev. Biol. 14*, 111−136.
44. Pike, L. J. (2003) Lipid rafts: bringing order to chaos, *J. Lipid Res. 44*, 655−667.
45. Fittipaldi, A., Ferrari, A., Zoppe, M., Arcangeli, C., Pellegrini, V., Beltram, F., and Giacca, M. (2003) Cell membrane lipid rafts mediate caveolar endocytosis of HIV-1 Tat fusion proteins, *J. Biol. Chem. 278*, 34141−34149.
46. Sandgren, S., Wittrup, A., Cheng, F., Jonsson, M., Eklund, E., Busch, S., and Belting, M. (2004) The human antimicrobial peptide LL-37 transfers extracellular DNA plasmid to the nuclear compartment of mammalian cells via lipid rafts and proteoglycan-dependent endocytosis, *J. Biol. Chem. 279*, 17951−17956.
47. Kauer, J. C., Erickson-Viitanen, S., Wolfe, H. R., Jr., and DeGrado, W. F. (1986) *p*-Benzoyl-L-phenylalanine, a new photoreactive amino acid. Photolabeling of calmodulin with a synthetic calmodulin-binding peptide, *J. Biol. Chem. 261*, 10695−10700.
48. Arap, M. A., Lahdenranta, J., Mintz, P. J., Hajitou, A., Sarkis, A. S., Arap, W., and Pasqualini, R. (2004) Cell surface expression of the stress response chaperone GRP78 enables tumor targeting by circulating ligands, *Cancer Cell 6*, 275−284.
49. Blond-Elguindi, S., Cwirla, S. E., Dower, W. J., Lipshutz, R. J., Sprang, S. R., Sambrook, J. F., and Gething, M.-J. H. (1993) Affinity panning of a library of peptides displayed on bacteriophages reveals the binding specificity of BiP, *Cell 75*, 717.
50. El-Andaloussi, S., Holm, T., and Langel, U. (2005) Cell-penetrating peptides: mechanisms and applications, *Curr. Pharm. Des. 11*, 3597−3611.
51. Misra, U. K., Gonzalez-Gronow, M., Gawdi, G., Hart, J. P., Johnson, C. E., and Pizzo, S. V. (2002) The role of Grp 78 in alpha 2-macroglobulin-induced signal transduction. Evidence from

RNA interference that the low-density lipoprotein receptor-related protein is associated with, but not necessary for, GRP 78-mediated signal transduction, *J. Biol. Chem. 277*, 42082−42087.
52. Misra, U. K., Deedwania, R., and Pizzo, S. V. (2005) Binding of activated alpha2-macroglobulin to its cell surface receptor GRP78 in 1-LN prostate cancer cells regulates PAK-2-dependent activation of LIMK, *J. Biol. Chem. 280*, 26278−26286.
53. Mintz, P. J., Kim, J., Do, K. A., Wang, X., Zinner, R. G., Cristofanilli, M., Arap, M. A., Hong, W. K., Troncoso, P., Logothetis, C. J., Pasqualini, R., and Arap, W. (2003) Fingerprinting the circulating repertoire of antibodies from cancer patients, *Nat. Biotechnol. 21*, 57−63.
54. Denmeade, S. R., and Isaacs, J. T. (2005) The SERCA pump as a therapeutic target−Making a "smart bomb" for prostate cancer, *Cancer Biol. Ther. 4*, 14−22.

BI060264J